ELSEVIER

Journal of Alloys and Compounds 458 (2008) 330–334

Journal of ALLOYS AND COMPOUNDS

www.elsevier.com/locate/jallcom

Hydrogen storage properties of melt-spun $LaNi_{4.25}Al_{0.75}$

H.H. Cheng [a,c], H.G. Yang [b], S.L. Li [a,c], X.X. Deng [a,c], D.M. Chen [a,*], K. Yang [a]

[a] *Institute of Metal Research, Chinese Academy of Sciences, Shenyang 110016, China*
[b] *China Institute of Atomic Energy, Beijing 102413, China*
[c] *Graduate School of Chinese Academy of Sciences, Beijing 100049, China*

Received 1 March 2007; received in revised form 19 March 2007; accepted 20 March 2007
Available online 30 March 2007

Abstract

Rapidly solidified $LaNi_{4.25}Al_{0.75}$ alloy was prepared by melt spinning and its hydrogen storage properties were examined. The hydrogen storage capacities and the equilibrium pressures of the unannealed melt-spun (UMS) $LaNi_{4.25}Al_{0.75}$ alloy were found to be nearly identical to those of the annealed induction-melt (AIM) alloy. However, the resistance to pulverization was greatly improved and the hysteresis was markedly decreased for the UMS alloy, while its activation became rather difficult.

Keywords: Hydrogen absorbing materials; Metal hydrides; Rare earth alloys and compounds; Gas–solid reactions; Rapid-solidification

1. Introduction

A lot of preparation methods, such as mechanical alloying [1], sputtering [2], gas-atomizing [3] and melt spinning [4], were attempted to acquire novel hydrogen storage properties for the hydrogen absorbing alloys. And some important conclusions have been made, e.g., the amorphous $LaNi_5$ alloys prepared by sputtering had lower hydrogen absorbing capacity [5]; it was difficult to obtain amorphous phases in $LaNi_5$ alloys [4]; the formation ability of amorphous phase in La–Ni–M (M = Si, Al, Mn, Co) system was in an order of Si > Al ≥ Mn > Co [6].

$LaNi_{4.25}Al_{0.75}$-tritide is used in the Savannah River Site (SRS) tritium processing facilities as the primary tritium storage medium, because the material is easily activated, a delivery pressure of 200 kPa is easily achieved by moderate heating, and it captures nearly the entire He formed from radiolytic decay of the solid tritide [7]. Since rapid quenching effect from molten metals induced by melt-spinning technique tends to alleviate the segregation in alloys, and to impel the alloys to form more lattice defects and grain boundaries [8], it was expected that this novel technique could introduce a positive effect on the hydrogen storage properties of $LaNi_{4.25}Al_{0.75}$ alloy, especially the long-term cyclic behavior.

2. Experimental

An ingot of the $LaNi_{4.25}Al_{0.75}$ alloy was prepared by a vacuum induction melting furnace under argon atmosphere. The purities of starting materials were: La 99.5%, Ni 99.9% and Al 99.7%. Afterwards, one part of the ingot was annealed as the reference at 1323 K for 8 h under argon atmosphere in a sealed quartz tube, while the other part was melt spun at a roller surface velocity of 39 m/s under a 400 mbar argon (99.99% purity) atmosphere. The temperature of the alloy for injection was about 1700 K. In order to investigate the long-term cycling effect, the $LaNi_{4.25}Al_{0.75}$ samples weighing about 1 g each were subjected to repetitious absorption/desorption cycles in an automatic Sieverts-type apparatus assembled with components from Swagelok® Company (USA) [9]. The detailed cyclic procedure was the same as that previously described [10]. The physical and structural properties of the powders were characterized by scanning electron microscopy (SEM), X-ray diffraction (XRD), and laser particle sizer, respectively.

3. Results and discussion

Fig. 1 shows an SEM image of the cross-section of the ribbon with thickness of 30–50 μm and width of 1–10 mm. It can be found that the melt-spun alloy has very fine grains and the ribbon mainly consists of columnar grains, which vertically grew up from the roller-contacting side. The diameter of each column is about 1–2 μm. A comparison of the first absorption/desorption

* Corresponding author. Tel.: +86 24 2397 1641; fax: +86 24 2389 1320.
E-mail address: demin.chen.1@imr.ac.cn (D.M. Chen).

0925-8388/$ – see front matter © 2007 Elsevier B.V. All rights reserved.
doi:10.1016/j.jallcom.2007.03.102

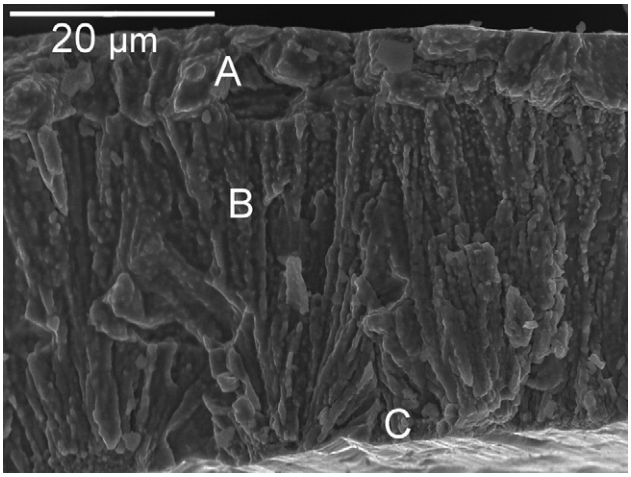

Fig. 1. SEM image of cross-section of the UMS-$LaNi_{4.25}Al_{0.75}$ ribbon: (A) equiaxial grain (free side), (B) columnar grain, and (C) nanocrystalline grain (roller side).

PC isotherms without pre-activation between the AIM alloy and the UMS alloy (Fig. 2) shows that the absorption plateau pressure of the latter is greatly higher than that of the former. This result suggests that the UMS alloy was more difficult to activate, which is consistent with the published electrochemical experimental results on melt-spun and gas-atomized AB_5 alloys [11,12]. In addition, it seems that as temperature increased, the activation process became enormously tougher. We did not find any evidence of hydrogen absorption with the UMS alloy even if the hydrogen pressure for activation was increased to about 4 MPa at 363 K. From Fig. 2, it also can be found that the residual hydrogen in the UMS alloy was more than that in the AIM alloy, which would be ascribed to the more stabilizing sites to accommodate hydrogen atoms in the alloy formed during melt spinning. Hence, the reversible capacity of the UMS alloy was less than that of the AIM alloy, which can also be validated in Table 1.

Fig. 3 shows the particle size distributions of the $LaNi_{4.25}Al_{0.75}$ alloys with absorption/desorption cycles. Volume mean diameter (VMD), which can be used to evaluate the pulverization degree, is a statistic value of a particle size distribution. From the VMD values of the two alloys, it can be concluded that melt spinning can greatly elevate the capability of pulverization resistance. The key influence can be from the lattice defects and grain boundaries, which work as the buffer regions for release of the lattice strain [8]. Fig. 4 indicates that there was a sharp contrast between the two morphologies of $LaNi_{4.25}Al_{0.75}$ particles after cycling. The fracture face of UMS-$LaNi_{4.25}Al_{0.75}$ particles seems parallel to the growth direction of columnar grain, which could be attributed to the different mechanical properties between the radial and axial directions of columnar grains. While the fracture faces of the AIM-$LaNi_{4.25}Al_{0.75}$ particles are randomly orientated.

Table 1
Degradation of the capacity

Sample	$C_0/C_{1000(1500)}$	k
AIM-$LaNi_{4.25}Al_{0.75}$ [10]	4.74/4.44	0.64×10^{-4}
UMS-$LaNi_{4.25}Al_{0.75}$	4.64/4.36	0.41×10^{-4}

Fig. 5 indicates that the UMS alloy has a homogeneous single $CaCu_5$-type structure and almost keeps this structure even after 1500 cycles. The average FWHM (full width at half maximum) of the main peaks for the UMS alloys, which was attained by using JADE software [13], was significantly larger than that of the AIM alloys. This is considered to be due to the lattice defects and/or small size grain boundaries introduced by melt spinning [8]. Fig. 6 shows the absorption/desorption PC isotherms of the UMS alloy after initial activation and 1500 absorption/desorption cycles, respectively. Comparing Fig. 6(a) and (b), it can be found that the capacity did not decrease significantly, about 6% capacity loss, after long-term cycles as that of the AIM alloy [10]. Mordkovich et al. [14] proposed the following empirical equation:

$$C_n = C_0 \exp(-kn) \quad (1)$$

where n presents the number of hydrogen absorption/desorption cycles, C_n the hydrogen capacity of the alloy after n hydro-

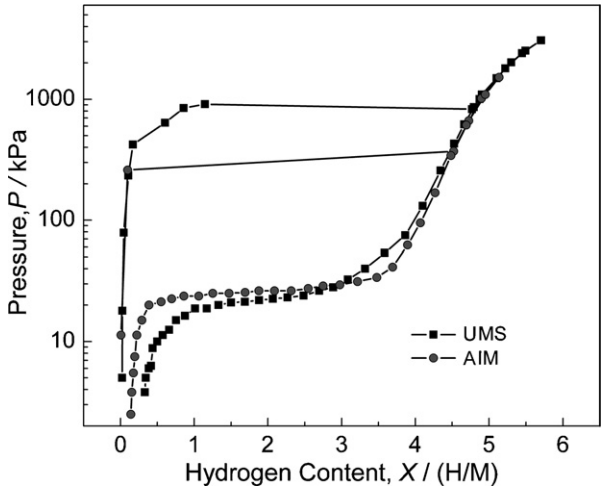

Fig. 2. Comparison of the first absorption/desorption PC isotherms of the $LaNi_{4.25}Al_{0.75}$ alloys at 353 K.

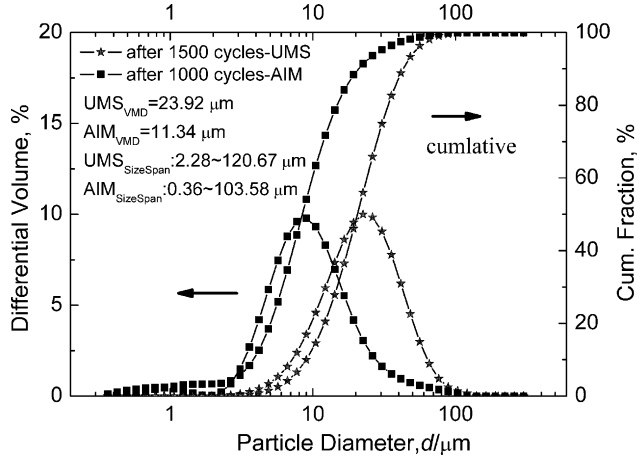

Fig. 3. Particle size distributions of the $LaNi_{4.25}Al_{0.75}$ alloys with absorption/desorption cycles.